Inorganic Chemistry

Article

pubs.acs.org/IC

3-D Silver(I)—Lanthanide(III) Heterometallic-Organic Frameworks Constructed from 2,2′-Bipyridine-3,3′-dicarboxylic Acid: Synthesis, Structure, Photoluminescence, and Their Remarkable Thermostability

Yunshan Zhou,* Xiaomin Li, Lijuan Zhang,* Yan Guo, and Zonghai Shi

State Key Laboratory of Chemical Resource Engineering, Institute of Science, Beijing University of Chemical Technology, Beijing 100029, P. R. China.

Supporting Information

ABSTRACT: A new family of silver(I)−lanthanide(III) heterometallic-organic frameworks having the formula $[AgLn(bpdc)_2]$ (Ln = Eu (**1**), Tb (**2**), Sm (**3**), Dy (**4**), Y (**5**), Yb (**6**), Er (**7**), Ho (**8**); H_2bpdc = 2,2′-bipyridine-3,3′-dicarboxylic acid), each of which crystallizes in the monoclinic space group $C2/c$ with $Z = 4$, has been hydrothermally synthesized. The compounds were characterized by means of IR, elemental analysis, thermogravimetric-differential thermal analysis, and powder X-ray diffraction (XRD), wherein compounds **1**, **2**, and **4**−**8** were structurally characterized. The powder XRD and single-crystal structures of the title compounds indicate that all the compounds are isostructural and feature a three-dimensional (3-D) open framework. In the structures of the compounds, $bpdc^{2-}$ ligands link Ln^{3+} through their carboxylic groups, resulting in the formation of a one-dimensional $\{Ln(bpdc)_2\}_n$ infinite chain along the c direction. The adjacent chains are then connected to each other through the coordination interaction between Ag^+ and the pyridyl N atoms of $bpdc^{2-}$ ligands from the chains, resulting in a 3-D (2,4,6)-connected open framework with $(4^{11}\cdot6^4)(4^3\cdot8^2\cdot10)(8)_2$ topology. The compounds show remarkable good thermally stability up to 370 °C because neither aquo ligands nor lattice water molecules exist in the composition of the compounds. The photoluminescent properties of compounds **1** and **2** were studied in detail. The energy level of the triplet states of the ligand H_2bpdc 21 505 cm^{-1} (465 nm) was determined based on the 77 K emission spectrum of the compound $[Gd_2(bpdc)_3(phen)_2(H_2O)_2]\cdot6H_2O$ **9**. The $^5D_0$ and $^5D_4$ emission lifetimes (1.58 and 1.76 ms) and the overall quantum yields (21% and 22%) were determined for the compounds **1** and **2**, respectively.

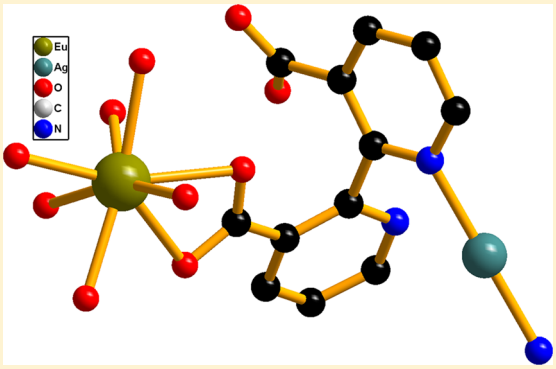

INTRODUCTION

Fluorescent lanthanide metal-organic frameworks (Ln-MOFs) have been of great interest due to their unique high fluorescence efficiencies, notable fluorescence monochromaticity, characteristic sharp emission, long excited-state luminescence lifetimes (up to milliseconds), and large Stokes shift (>200 nm).[1] Therefore, Ln-MOFs are excellent candidates for the development of light-emitting diodes, sensors, fluorescent probes in biochemistry, determination of the trace amounts of lanthanide ions in solution, and electroluminescent optical devices.[2] In this context, trivalent lanthanide metal cations like Eu^{3+}, Tb^{3+}, Sm^{3+}, and Dy^{3+} exhibit high color purity and fluorescent efficiency and are fascinating luminescent sources, whereas they usually suffer from weak light absorption due to the forbidden f→f transitions (Laporte forbidden), making the direct excitation of the metal ions very inefficient and inappropriate for their applications.[3] This problem can be overcome by coupling organic ligands that can participate in energy transfer processes, known as "luminescence sensitization" or "antenna effect".[4] Previous studies indicated that the ligands with rigid and conjugate structures can sensitize luminescence of lanthanide ions.[5] At present, it is reported that β-diketonates[6] and aromatic carboxylic acids[7] were often employed as the sensitizers for the luminescence of lanthanide ions. In addition, it was reported that the introduction of a transition metal in lanthanide complexes can enhance the luminescence of the lanthanide complexes,[8] because the transition metal has a small coordination number, which helps to decrease the steric hindrance around the Ln^{3+} in the 3d−4f or 4d−4f heterometallic complexes, preventing the solvent molecules from coordination to Ln^{3+} and accordingly enhance the luminescence intensity of the complexes.[9] Some investigations have shown that Ag^+ ion ($4d^{10}$) having a special closed outer shell electron configuration can provide a way to achieve novel heterometallic complexes with beautiful architectures and improved luminescent properties of the resulting Ag−Ln heterometallic complexes.[10−13] A typical

Received: October 29, 2013
Published: March 17, 2014

   dx.doi.org/10.1021/ic402718c | Inorg. Chem. 2014, 53, 3362−3370

strategy to construct Ag−Ln heterometallic MOFs lies in selecting proper ligands containing both oxygen and nitrogen atoms, such as nicotinic acid,[10d,e] isonicotinic acid,[10a,b,d,f] or pyrazine-2-carboxylate.[10] As a consequence, so far several Ag−Ln compounds based on these kind of ligands have been reported with one-dimensional (1-D)[13,14] and two-dimensional (2-D)[10e,15,16] structures; however three-dimensional (3-D) frameworks structures of Ag−Ln MOFs are rarely acquired successfully,[10b−f] probably due to the low coordination number of Ag^+ and the ligands used having low chelating positions. Therefore searching for multifunctional ligands possessing more coordinating sites still remains a challenge to construct 3-D Ag−Ln MOFs.

From the viewpoint of the analysis above, we have considerable interest in the use of multifunctional organic ligands containing multioxygen and nitrogen atoms to construct 3-D Ag−Ln heterometallic MOFs. In this context, 2,2′-bipyridine-3,3′-dicarboxylic acid (H_2bpdc) (Scheme 1) is a

Scheme 1. The Structure of 2,2′-Bipyridine-3,3′-dicarboxylic acid (H_2bpdc)

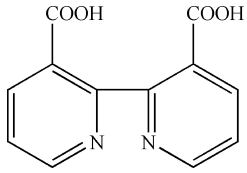

typical multidentate N and O donor ligand,[17] featuring the strong chelating bipyridyl moiety and the adjacent carboxyl groups. In previous studies,[21−23] $bpdc^{2-}$ often plays a role as a bis(monodentate),[18] tridentate,[19] bis(bidentate),[20] pentadentate,[21] or even hexadentate[21,22] bridge-connecter, which can facilitate and/or direct the formation of MOFs. Additionally, the bonding of bipyridyl and carboxyl groups of $bpdc^{2-}$ to the selected metal centers may greatly twist the configuration of $bpdc^{2-}$ along the 1,10-bond, which may provide a route for metal-directed self-assembly.[23] Therefore, from the standpoint of the analysis of the $bpdc^{2-}$ ligand, collaboration of Ag^+ ion with Ln^{3+} ion may offer a way to construct 3-D Ag−Ln MOFs with promising structures and interesting luminescent properties. Herein, we report on the preparation, structures and photoluminescent properties of a new family of 3-D Ag−Ln heterometallic MOFs, [AgLn(bpdc)$_2$] (Ln = Eu (**1**), Tb (**2**), Sm (**3**), Dy (**4**), Y (**5**), Yb (**6**), Er (**7**), Ho (**8**)) using the versatile ligand 2, 2′-bipyridine-3, 3′-dicarboxylic acid (H_2bpdc).

EXPERIMENTAL DETAILS

Materials and Method. H_2bpdc was synthesized according to a literature method previously reported[24] and characterized by IR, UV−visible, and elemental analysis. Anal. Calcd for $C_{12}H_8N_2O_4$ (H_2bpdc): C, 59.05; H, 3.23; N, 11.51. Found: C, 59.02; H, 3.28; N, 11.48%. IR (KBr, cm^{-1}): 2902(s), 1719 (s), 1585(s), 1430 (s), 1151(s). All other materials and solvents, obtained from commercial sources, were of reagent grade and used without further purification. IR spectra were recorded on a Nicolet FTIR-170SX spectrometer in a KBr pellet, in the range of 4000−400 cm^{-1}. Elemental analyses for C, H, and N were performed on a Perkin-Elmer 240C analytical instrument, while analyses for Ag, Eu, Tb, Sm, Dy, Y, Yb, Er, and Ho in all samples, which were dissolved in dilute hydrochloric acid, were carried out by using an ICPS-7500 model inductively coupled plasma emission spectrometer (ICP-ES). The UV−vis spectra were recorded on a Shimadzu UV-2550 spectrophotometer in the range of 200−800 nm. Powder X-ray diffraction (XRD) measurements were carried out on a Rigaku D/max 2500 X-ray diffractometer with a graphite-monochromatized Cu Kα line (λ = 0.154 05 nm) as the incident beam. The scanning rate was set to 15°/min in the 2θ range from 3° to 90°. Thermogravimetric analyses were carried out on a NETZSCH STA 449C unit at a heating rate of 10 °C/min. The excitation and emission spectra were measured with a Hitachi F-7000 FL fluorescence spectrophotometer. Both excitation and emission slits of 5 nm were set in solid-state photoluminescence measurement for compounds **1** and **2** using a xenon arc lamp (150 W) as the light source. The scan speed is 1200 nm/min, and PMT voltage is 400 V. The low-temperature phosphorescence spectra for compound [Gd_2(bpdc)$_3$-(phen)$_2$(H_2O)$_2$]·6H_2O **9** in solid state were measured with a Hitachi F-7000 FL fluorescence spectrophotometer with emission slit of 5 nm; the scan speed is 240 nm/min, and PMT voltage is 700 V using a xenon arc lamp (150 W) as the light source. The photoluminescence quantum yields of the samples were obtained using an Absolute PL Quantum Yield measurement system C9920−02. A Lecroy Wave Runner 6100 Digital Oscilloscope (1 GHz) was used to obtain the luminescence decay curves of the samples using a tunable laser with pulse width of 4 ns and gate of 50 ns as the excitation (Contimuum Sunlite OPO).

Synthesis of [AgEu(bpdc)$_2$] 1. A mixture of H_2bpdc (0.5 mmol, 0.122 g), Eu_2O_3 (0.25 mmol, 0.088 g), $AgNO_3$ (0.1 mmol, 0.017 g), and H_2O (10 mL) was placed in a 23 mL Teflon-lined stainless steel vessel and was kept under autogenous pressure at 170 °C for 3 d and then slowly cooled to room temperature at the rate 10 °C per hour. Colorless tubular-shape single crystals (Supporting Information, Figure S1) were obtained, with yield of 65.7% based on Ag. Anal. Calcd (%) for $C_{24}H_{12}AgEuN_4O_8$: C, 38.68; H, 1.64; N, 7.55; Ag, 14.49; Eu, 20.42. Found: C, 38.71; H, 1.61; N, 7.53; Ag, 14.40; Eu, 20.28. IR (KBr, cm^{-1}): 3445(v), 3095(v), 1656(s), 1594(s), 1552(s), 1445(s), 1416(s), 1369(s), 1348(s), 1156(m), 1098(m), 864(m), 770(s), 697(m), 634(v), 603(v), 431(m).

Synthesis of [AgTb(bpdc)$_2$] 2. The compound was synthesized in a manner similar to that for compound **1**, except that Tb_4O_7 was used instead of Eu_2O_3 (0.125 mmol, 0.093 g). Colorless tubular-shape crystals were obtained, with yield of 65.3% based on Ag. Anal. Calcd (%) for $C_{24}H_{12}AgTbN_4O_8$: C, 38.33; H, 1.59; N, 7.50; Ag, 14.36; Tb, 21.16. Found: C, 38.35; H, 1.60; N, 7.46; Ag, 14.45; Tb, 21.08. IR (KBr, cm^{-1}): 3445(v), 3091(v), 1662(s), 1599(s), 1552(s), 1448(s), 1422(s), 1375(s), 1354(s), 1156(m), 1103(m), 874(m), 770(s), 697(m), 629(v), 598(v), 431(m).

Synthesis of [AgSm(bpdc)$_2$] 3. The compound was synthesized in a manner similar to compound **1** except that Eu_2O_3 was replaced by Sm_2O_3 (0.25 mmol, 0.087 g). Colorless tubular-shape crystals were obtained, with yield of 64.2% based on Ag. Anal. Calcd for $C_{24}H_{12}AgSmN_4O_8$: C, 38.75; H, 1.64; N, 7.57; Ag, 14.53; Sm, 20.25. Found: C, 38.76; H, 1.62; N, 7.55; Ag, 14.48; Sm, 20.29%. IR (KBr, cm^{-1}): 3440(v), 3091(v), 1656(s), 1598(s), 1552(s), 1448(s), 1416(s), 1368(s), 1348(s), 1156(m), 1078(m), 869(m), 775(s), 697(m), 634(v), 582(v), 431(m).

Synthesis of [AgDy(bpdc)$_2$] 4. The compound was synthesized in a manner similar to compound **1** except that Eu_2O_3 was replaced by Dy_2O_3 (0.25 mmol, 0.093 g). Colorless tubular-shape crystals were obtained, with yield of 64.6% based on Ag. Anal. Calcd for $C_{24}H_{12}AgDyN_4O_8$: C, 38.16; H, 1.62; N, 7.47; Ag, 14.29; Dy, 21.53. Found: C, 38.20; H, 1.59; N, 7.43; Ag, 14.35; Dy, 21.40%. IR (KBr, cm^{-1}): 3445(v), 3091(v), 1656(s), 1599(s), 1552(s), 1448(s), 1422(s), 1386(s), 1354(s), 1156(m), 1103(m), 872(m), 775(s), 691(m), 629(v), 598(v), 436(m).

Synthesis of [AgY(bpdc)$_2$] 5. The compound was synthesized in a manner similar to compound **1** except that Eu_2O_3 was replaced by Y_2O_3 (0.25 mmol, 0.056 g). Colorless tubular-shape crystals were obtained, with yield of 65.0% based on Ag. Anal. Calcd for $C_{24}H_{12}AgYN_4O_8$: C, 42.31; H, 1.74; N, 8.19; Ag, 15.83; Y, 13.05. Found: C, 42.29; H, 1.72; N, 8.22; Ag, 15.90; Y, 13.21%. IR (KBr, cm^{-1}): 3429(v), 3091(v), 1662(s), 1599(s), 1552(s), 1443(s), 1422(s), 1380(s), 1354(s), 1150(m), 1108(m), 874(m), 770(s), 697(m), 639(v), 592(v), 436(m).

dx.doi.org/10.1021/ic402718c | Inorg. Chem. 2014, 53, 3362−3370

Table 1. Crystal Data and Structure Refinement for the Compounds 1, 2, and 4−8

identification code	1	2	4	5	6	7	8
empirical formula	$C_{24}H_{12}AgEuN_4O_8$	$C_{24}H_{12}AgTbN_4O_8$	$C_{24}H_{12}AgDyN_4O_8$	$C_{24}H_{12}AgN_4O_8Y$	$C_{24}H_{12}AgN_4O_8Yb$	$C_{24}H_{12}AgErN_4O_8$	$C_{24}H_{12}AgHoN_4O_8$
formula weight	744.21	751.17	754.75	681.16	765.29	759.51	757.18
temperature, K	301(2)	102(2)	301(2)	293(2)	293(2)	293(2)	293(2)
crystal system	monoclinic	monoclinic	monoclinic	monoclinic	Monoclinic	monoclinic	monoclinic
space group	*C*2/*c*	*C*2/*c*	*C*2/*c*	*C*2/*c*	*C*2/*c*	*C*2/*c*	*C*2/*c*
a/Å	24.4855(8)	24.5330(1)	24.5101(14)	24.5212(15)	24.615(5)	24.5295(8)	24.520(2)
b/Å	12.1360(4)	12.084.(6)	12.1342(11)	12.1479(8)	12.0995(11)	12.1210(5)	12.1514(7)
c/Å	7.4943(3)	7.4465(4)	7.4571(4)	7.4313(4)	7.3686(3)	7.4131(3)	7.4337(3)
α/deg	90.00	90.00	90.00	90.00	90.00	90.00	90.00
β/deg	93.055(3)	93.073(4)	93.302(5)	93.329(5)	93.350(7)	93.319(3)	93.212(4)
γ/deg	90.00	90.00	90.00	90.00	90.00	90.00	90.00
volume/Å^3	2223.82(13)	2204.40(18)	2214.1(3)	2209.9(2)	2190.8(5)	2200.39(13)	2211.5(3)
Z	4	4	4	4	4	4	4
ρ_{calc}/mg/mm^3	2.223	2.263	2.264	2.047	2.320	2.293	2.274
μ/mm^{-1}	3.738	4.134	25.507	3.563	5.200	4.741	4.501
F(000)	1432	1440	1444	1336	1460	1452	1448
crystal size/mm^3	0.40 × 0.40 × 0.50	0.40 × 0.07 × 0.07	0.50 × 0.11 × 0.07	0.80 × 0.40 × 0.25	0.08 × 0.15 × 0.30	0.10 × 0.20 × 0.50	0.30 × 0.60 × 0.07
reflections collected	7604	4625	3774	4318	7232	4903	4753
independent reflections	1999[*R*(int)= 0.0627]	2163[*R*(int)= 0.0278]	1988[*R*(int)= 0.0335]	2169[*R*(int)= 0.0220]	2151[*R*(int)= 0.0353]	2161[*R*(int)= 0.0395]	2170[*R*(int)= 0.0227]
goodness-of-fit on F^2	1.059	1.036	0.955	1.053	1.072	1.053	1.083
$R1^a$ [$I \geq 2\sigma(I)$]	0.0283	0.0263	0.0319	0.0284	0.0218	0.0300	0.0211
$wR_2{}^b$ [$I \geq 2\sigma(I)$]	0.0651	0.0576	0.0792	0.0677	0.0485	0.0611	0.0506
CCDC No.	968582	968576	968581	968577	968580	968578	968579

$^a R1 = \Sigma||F_o| - |F_c||/\Sigma|F_o|$. $^b wR_2 = \Sigma[w(F_o{}^2 - F_c{}^2)^2]/\Sigma[w(F_o{}^2)^2]^{1/2}$.

dx.doi.org/10.1021/ic402718c | *Inorg. Chem.* 2014, 53, 3362−3370

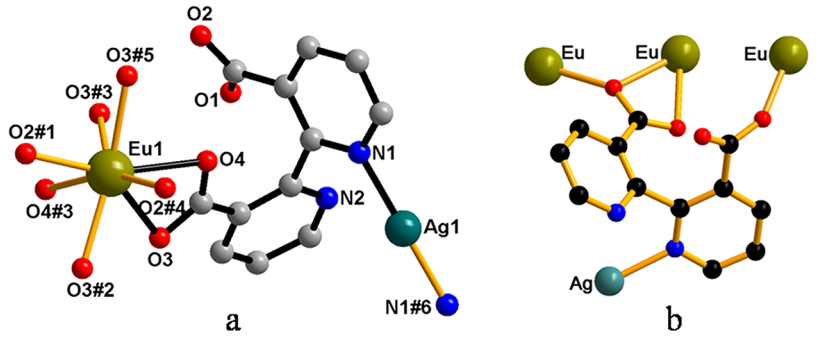

Figure 1. (a) The coordination environment around Eu^{3+} and Ag^{+} in complex **1**, with labeling scheme wherein atoms composing the asymmetric unit are connected by black-filled bonds. (b) The coordination mode of $bpdc^{2-}$ in compound **1**. Hydrogen atoms have been omitted for clarity. Color code: C, gray; Eu, olive; N, blue; O, red; Ag, teal. Symmetry transformations used to generate equivalent atoms: #1, 1 − x, 1 − y, −z; #2, 1 − x, 1 − y, 1 − z; #3, 1 − x, +y, 1/2 − z; #4, +x, 1 − y, 1/2 + z; #5, +x, 1 − y, −1/2 + z; #6, 3/2 − x, 1/2 − y, 1 − z.

Synthesis of $[AgYb(bpdc)_2]$ 6. The compound was synthesized in a manner similar to compound **1** except that Eu_2O_3 was replaced by Yb_2O_3 (0.25 mmol, 0.098 g). Colorless tubular-shaped crystals were obtained, with yield of 61.0% based on Ag. Anal. Calcd for $C_{24}H_{12}AgYbN_4O_8$: C, 37.68; H, 1.55; N, 7.37; Ag, 14.09; Yb, 22.61. Found: C, 37.65; H, 1.57; N, 7.32; Ag, 13.97; Yb, 22.68%. IR (KBr, cm^{-1}): 3424(v), 3096(v), 1663(s), 1600(s), 1553(s), 1449(s), 1417(s), 1381(s), 1360(s), 1157(m), 1084(m), 870(m), 771(s), 703(m), 630(v), 599(v), 432(m).

Synthesis of $[AgEr(bpdc)_2]$ 7. The compound was synthesized in a manner similar to compound **1** except that Eu_2O_3 was replaced by Er_2O_3 (0.25 mmol, 0.095 g). Light pink tubular-shaped crystals were obtained, with yield of 68.0% based on Ag. Anal. Calcd for $C_{24}H_{12}AgErN_4O_8$: C, 37.91; H, 1.62; N, 7.35; Ag, 14.20; Er, 22.02. Found: C, 37.94; H, 1.58; N, 7.38; Ag, 14.11; Er, 22.15%. IR (KBr, cm^{-1}): 3440(v), 3086(v), 1657(s), 1600(s), 1552(s), 1440(s), 1417(s), 1370(s), 1346(s), 1152(m), 1108(m), 870(m), 771(s), 703(m), 630(v), 594(v), 432(m).

Synthesis of $[AgHo(bpdc)_2]$ 8. The compound was synthesized in a manner similar to compound **1** except that Eu_2O_3 was replaced by Ho_2O_3 (0.25 mmol, 0.094 g). Flaxen tubular-shape crystals were obtained, with yield of 66.0% based on Ag. Anal. Calcd for $C_{24}H_{12}AgHoN_4O_8$: C, 38.06; H, 1.64; N, 7.45; Ag, 14.25; Ho, 21.78. Found: C, 38.10; H, 1.59; N, 7.41; Ag, 14.31; Ho, 21.85%. IR (KBr, cm^{-1}): 3440(v), 3095(v), 1662(s), 1599(s), 1552(s), 1448(s), 1416(s), 1375(s), 1354(s), 1161(m), 1078(m), 874(m), 775(s), 697(m), 634(v), 592(v), 431(m).

Synthesis of Microtubes of $[Ag(2,2'\text{-bipyridine})]NO_3{\cdot}5H_2O$. The compound was synthesized in a manner similar to compound **1** except that the dosage of $AgNO_3$ was doubled (0.2 mmol, 0.034 g) in the mixture. Any Ln_2O_3 can be used in the mixture, and a large amount of pale yellow microtubes (Supporting Information, Figure S2) can be obtained, with yield of 69.0% based on $AgNO_3$. Anal. Calcd for $C_{24}H_{26}AgN_5O_8$: C, 46.46; H, 4.22; N, 11.29; Ag, 17.38. Found: C, 46.88; H, 4.02; N, 11.44; Ag, 17.29%. IR (KBr, cm^{-1}): 3444(v), 3060(v), 1582(s), 1557(s), 1456(s), 1386(s), 1253(s), 1040(s), 994(m), 757(s), 620(m) (Supporting Information, Figure S3).

Synthesis of $[Gd_2(bpdc)_3(phen)_2(H_2O)_2]{\cdot}6H_2O$ 9. This compound was synthesized according to a literature method previously reported.[25] The characterization of the compound was carried out by elemental analysis, IR, and XRD (Supporting Information, Figure S4) approaches. Anal. Calcd. for $C_{60}H_{50}Gd_2N_{10}O_{20}$: C, 46.56; H, 3.25; N, 9.03. Found: C, 46.46; H, 3.24; N, 8.96%. IR (KBr, cm^{-1}): 3372(m), 1584(s), 1543(s), 1455(m), 1393(s), 1163(m), 1079(m), 858 (m) cm^{-1}.

X-ray Crystallography. Single-crystal X-ray diffraction data for the compounds were collected on a Bruker APEX2 X-Diffraction instrument equipped with Mo Kα radiation (λ = 0.71073 Å) in the ω scan mode. The structures were solved by direct methods and by subsequent successive difference Fourier syntheses with the SHELX 97 program package.[26,27] All of the non-H atoms were refined with anisotropical displacement coefficients. H atoms were added to a model in their geometrically ideal positions. A summary of the crystallographic data and structural determination parameters of the compounds **1**, **2**, and **4**−**8** are given in Table 1, and the selected bond lengths and bond angles of compound **1** selected as a representative sample are listed in Supporting Information, Table S1.

RESULTS AND DISCUSSION

Hydrothermal Synthesis of Compounds 1−8. Reaction conditions always decide the results of chemical reactions. It was found that a large amount of tubular-shaped single crystals of the compounds **1**−**8** could be harvested when the molar ratio of the starting materials $H_2bpdc/Eu_2O_3/AgNO_3$ was 0.5:0.25:0.1 at 160−170 °C for 3−6 d followed by cooling with rate of 1−15 °C/h. When the dosage of $AgNO_3$ was ≥0.10 mmol, pale yellow microtubes confirmed as $[Ag(2,2'\text{-bipyridine})]NO_3{\cdot}5H_2O$ were obtained (Supporting Information, Figure S2). On the basis of the experimental result, a conclusion could be made that the molar ratio of the selected starting materials is more important than the cooling rate and the reaction time for the preparation of compounds **1**−**8**. For the synthesis of compound **2**, although the starting material is Tb_4O_7, which is different from the others (Ln_2O_3), the final composition and structure are the same as the others. A redox reaction happened somehow under the experimental conditions.

Powder XRD Patterns. As shown in Supporting Information, Figure S5, the powder XRD patterns of the compounds **1**−**8** are in good agreement with those calculated from single-crystal X-ray diffraction data, indicating that the phases of the final products are homogeneous. No further byproduct in the products was identified. The essential agreement of powder XRD patterns confirms that compounds **1**−**8** are isomorphous, which is consistent with the single-crystal X-ray diffraction analysis described below.

Structures of the Compounds 1, 2, and 4−8. According to the results of powder X-ray diffraction and single-crystal X-ray analysis, the eight Ag−Ln heterometallic compounds, namely, $[AgLn(bpdc)_2]$ (Ln = Eu (**1**), Tb (**2**), Sm (**3**), Dy (**4**), Y (**5**), Yb (**6**), Er (**7**), and Ho (**8**)), are isostructural and crystallize in monoclinic space group $C2/c$; therefore, only compound **1** is selected as a representative to depict the structural details.

In the asymmetric unit of compound **1**, there are 0.5 Eu^{3+} ion, 0.5 Ag^{+} ion, and one $bpdc^{2-}$ ligand, which are crystallographically independent. The Eu^{3+} ion is 8-coordinated with eight oxygen atoms (O3, O4, O3#3 and O4#3, O2#1,

dx.doi.org/10.1021/ic402718c | Inorg. Chem. 2014, 53, 3362−3370

O3#2, O2#4, and O3#5) from carboxylic groups of six different $bpdc^{2-}$ ligands (Figure 1a). The Eu−O bond lengths are in the range of 2.232(3)−2.527(3) Å, and the O−Eu−O bond angles are in the range of 51.80(9)−161.95(10)°, which are similar to those in the reported Eu complexes.[2] Remarkably, no aquo ligand appears in the coordination environment of Eu(III) in compound **1**, while Ln^{3+} ions are all coordinated with water molecules in the reported Ln-MOFs composed of $bpdc^{2-}$ ligands.[28] The Ag^{+} ion is 2-coordinate, with two nitrogen atoms (N1 and N1#6) of pyridyl groups from two different $bpdc^{2-}$ ligands (Figure 1a). The Ag−N bond distance is 2.137(4) Å, and the N−Ag−N bond angle is 180°, which are also comparable to those in the literature.[10b] The $bpdc^{2-}$ ligands adopt a tetraconnected coordination mode in which two carboxylate groups of one $bpdc^{2-}$ ligand take the bridging mode to connect three Eu^{3+} (Figure 1b) while two nitrogen atoms of one $bpdc^{2-}$ ligand connect one Ag^{+}.

As illustrated in Figure 2a, the adjacent Eu^{3+} ions are linked by $bpdc^{2-}$ ligands through their carboxylic groups to form a 1-D infinite chain along the *c* direction, in which the neighboring Eu···Eu distance is 3.9941(2) Å. Then, the neighboring 1-D chains are linked by the Ag^{+} ions by coordinating to the nitrogen atoms of the pyridine rings of $bpdc^{2-}$ ligands from the chains to form a 2-D layer in the *ac* plane (Figure 2b). The shortest Eu···Eu distance between the adjacent 1-D infinite chains within the 2-D layer is 13.6640(4) Å. The adjacent 2-D layers are further joined together via the coordination interactions of pyridyl nitrogen atoms of $bpdc^{2-}$ of the adjacent layers and Ag^{+}, resulting in a 3-D open framework with 1-D rhombic channels with the side length being 13.6640(4) Å based on the shortest Eu···Eu distance (Figure 2c).

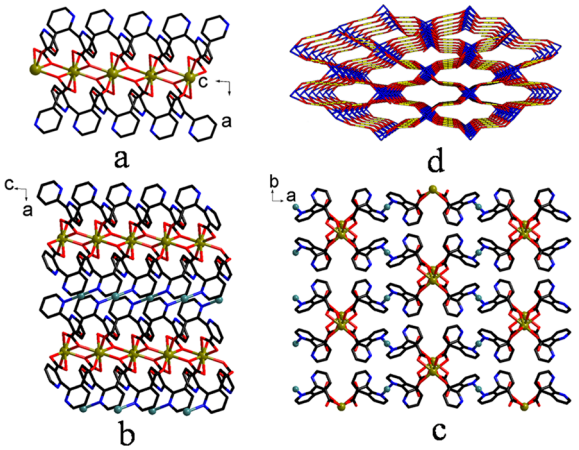

Figure 2. The 1-D chain along *c* direction in compound **1** (a); the 2-D layer composed of the 1-D chains in the *ac* plane in compound **1** (b); the 3-D open framework structure composed of 2-D layers in compound **1** (c); and topos structure with $(4^{11}\cdot6^{4})(4^{3}\cdot8^{2}\cdot10)(8)_2$ topology in *c* direction in compound **1** (d). Color code: C, black; Eu, olive; N, blue; O, red; Ag, teal in (a), (b), and (c). Six-connected Eu^{3+} ion, blue node, four-connected $bpdc^{2-}$ ligand, red node; two-connected Ag^{+}, yellow node. All H atoms were omitted for clarity.

Topological analysis on the 3-D structure of compound **1** was carried out. In the structure, each Eu^{3+} ion links six $bpdc^{2-}$ ligands and therefore is regarded as a hexacorner-share holder; each Ag^{+} ion links two $bpdc^{2-}$ ligands and therefore is regarded as a bicorner-share holder, and each $bpdc^{2-}$ ligand is regarded as a quadcorner-share holder. As shown in Figure 2d, the connectivity of these holders in compound **1** results in the 3-D framework featuring a trinodal (2,4,6)-connected net with Point (Schläfli) symbol of $(4^{11}\cdot6^{4})(4^{3}\cdot8^{2}\cdot10)(8)_2$.[29]

IR Spectra of the Free Ligand and Compounds 1−8. In the IR spectrum of the free ligand H_2bpdc (Supporting Information, Figure S6), the strong band at 3089 cm^{-1} can be attributed to the =C−H stretching vibrations of the pyridine rings.[30] The O−H stretching vibrations of the carboxylic groups are reflected by the appearance of a broad band in the range of 3200−2300 cm^{-1} centered at 2902 cm^{-1}.[31] The strong band centered at 1719 cm^{-1} arises from the stretching vibrations of the C=O bond from carboxylic groups of the ligand.[32] The stretching vibrations of the C=N bond from the pyridine ring of the ligand is observable from the appearance of the band at 1585 cm^{-1}.[33] Furthermore, the two strong bands at 1430 and 1151 cm^{-1} are due to the characteristic vibrational frequencies of the pyridine ring.[34]

Because the IR spectra (see Supporting Information, Figure S6) of compounds **1**−**8** are almost the same, reflecting their isomorphous nature, the spectrum of compound **1** is selected as a representative for interpretation. Compared with H_2bpdc, in the IR spectrum of compound **1**, the absence of a broad band in the range of 3200−2300 cm^{-1} and the strong band at 1719 cm^{-1}, assigned to the carboxylic groups, and the presence of the characteristic bands of carboxylate groups at 1594 cm^{-1} for asymmetric stretching and at 1416 cm^{-1} for symmetric stretching vibration indicate that, in the reaction process, the H_2bpdc ligand is deprotonated and then bridges the Eu^{3+} ions through coordination action, which is in agreement with the single-crystal X-ray structure of compound **1**.[35]

UV−vis Absorption Spectrum of H_2bpdc. As shown in Figure 3, the UV−vis absorption spectrum of H_2bpdc in dimethylformamide (DMF) shows one UV−vis absorption band at 266 nm, which is assigned to the $\pi\rightarrow\pi^*$ transition of H_2bpdc.[1,36] On the basis of the molar extinction coefficient value of the ligand at 266 nm being 5.6×10^{3} $L\cdot mol^{-1}\cdot cm^{-1}$, it is known that the ligand is a good light-harvesting chromophore to sensitize lanthanide luminescence.[37] The singlet-state energy level of H_2bpdc is calculated to be 34 014 cm^{-1} (294 nm) on the basis of UV−vis absorption spectrum absorbance edge[38] of H_2bpdc.

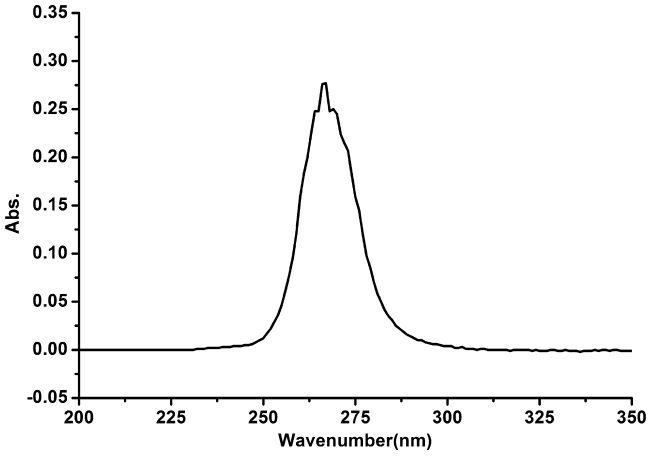

Figure 3. The UV−vis absorption spectrum of H_2bpdc (5×10^{-5} M) in DMF.

Diffuse Reflectance Spectroscopy. The free ligand H_2bpdc shows an absorption band at 288 nm in the UV region of its diffuse reflectance spectrum (see Figure 4), which

dx.doi.org/10.1021/ic402718c | Inorg. Chem. 2014, 53, 3362−3370

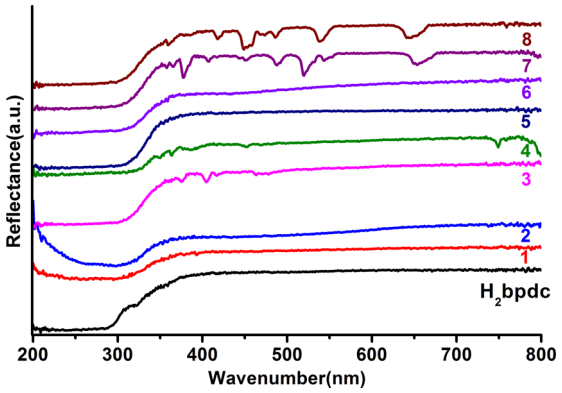

Figure 4. Solid-state diffuse reflectance spectra of the free ligand H_2bpdc (black line) and compounds **1** (red), **2** (blue), **3** (pink), **4** (green), **5** (dark blue), **6** (light purple), **7** (purple), and **8** (brown).

is assigned to the $\pi\rightarrow\pi^*$ transition of the ligand.[1,32,36] The spectra of compounds **1**−**8** are similar to the one observed for the free ligand H_2bpdc. This means that the complexation of the Ln^{3+} ion does not affect remarkably the singlet excited state of the free ligand.[1] The characteristic intra-4f^n transitions of Ln^{3+} are also observed for compounds **3**, **4**, **7**, and **8**. As compared to the free ligand, a small red shift in the absorption maximum of the compounds indicates an effective interaction between the lanthanide cations and the organic ligand.[39] On the basis of the above result, the observed band in the UV region of diffuse reflectance spectra for compounds **1**−**8** and for the ligand are thought to correspond to electronic transitions from the ground state level S_0 to the excited state level S_1 of H_2bpdc.

Photoluminescence Properties. Since the lowest excited state $^6P_{7/2}$ of Gd(III) ion is too high to accept energy from a ligand, the triplet energy level of the corresponding ligand can be obtained from the phosphorescence spectrum of its Gd(III) complex.[40] In the case of the mixed-ligand complex $[Gd_2(bpdc)_3(phen)_2(H_2O)_2]\cdot 6H_2O$ **9**, two well-defined phosphorescence bands, peaking around 453 and 465 nm, are observed in the low-temperature (77 K) phosphorescence spectrum (Figure 5) and are ascribed to the triplet levels of the H_2bpdc and phen ligands, respectively. One of the triplets at 22 100 cm^{-1} (453 nm) is attributed to the phen ligand,[41] so the other triplet state energy ($^3\pi\pi^*$) level at 21 505 cm^{-1} (465 nm)

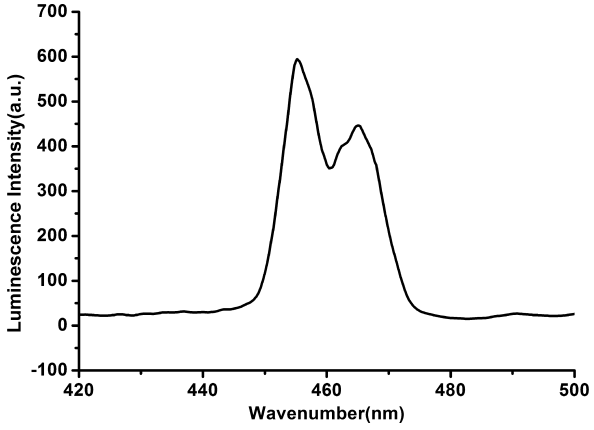

Figure 5. The phosphorescence spectrum of $[Gd_2(bpdc)_3(phen)_2(H_2O)_2]\cdot 6H_2O$ at 77K.

is due to the H_2bpdc ligand.[42] As it is known that the intersystem crossing process becomes effective when $\Delta E(^1\pi\pi^*-^3\pi\pi^*)$ of the ligand is over at least 5000 cm^{-1},[37] the energy gap between the $^1\pi\pi^*$ (34 014 cm^{-1}) and $^3\pi\pi^*$ (21 505 cm^{-1}) levels being 12 509 cm^{-1} for H_2bpdc indicates effective intersystem crossing process in the title compounds.

The energy differences (Scheme 2) between the lowest triplet state of H_2bpdc and the resonant energy levels of Eu^{3+}

Scheme 2. The Singlet and Triplet Energy Levels of H_2bpdc Ligand, Energy Differences between Ln^{3+} Ions and H_2bpdc Ligand in Compounds 1−4, Energy Level Diagram, and the Schematic Energy Transfer Process in Compounds 1−4

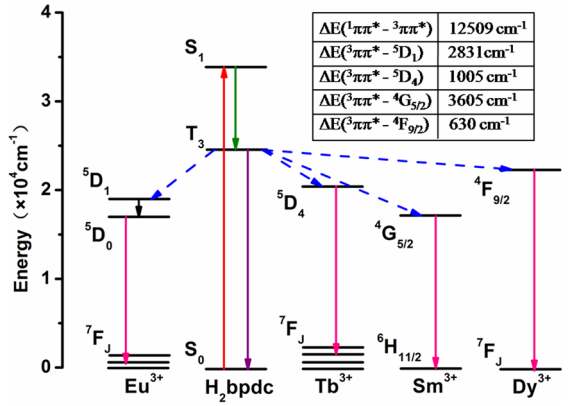

($^5D_1$, 18 674 cm^{-1}), Tb^{3+} ($^5D_4$, 20 500 cm^{-1}), Sm^{3+} ($^4G_{5/2}$, 17 900 cm^{-1}) and Dy^{3+} ($^4F_{9/2}$, 20 875 cm^{-1}) are 2831 cm^{-1}, 1005 cm^{-1}, 3605 cm^{-1}, and 630 cm^{-1}, respectively. As it is known[43] that an optimal ligand-to-metal energy transfer process for Ln(III) needs 2500−3500 cm^{-1} for Eu(III) and 2500−4500 cm^{-1} for Tb(III), the energy differences seen in Scheme 2 therefore show that the transitions from the triplet energy level of H_2bpdc to Eu^{3+} and Tb^{3+} are effective; that is, H_2bpdc is a suitable sensitizer for the luminescence of Eu^{3+} and Tb^{3+} rather than for Sm^{3+} and Dy^{3+}.

The solid-state excitation and emission spectra recorded at room temperature for compounds **1** and **2** are depicted in Figures 6 and 7, respectively. The excitation spectrum (Figure 6a) of compound **1** monitored the intense characteristic emission (615 nm) of the Eu^{3+} ion and displays a prominent

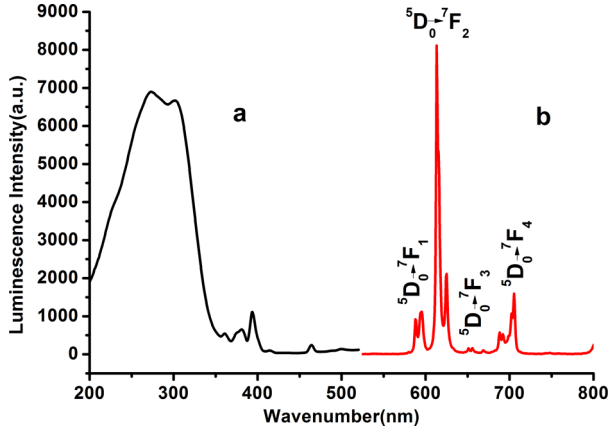

Figure 6. The solid-state excitation (λ_{em} = 615 nm) (a) and emission (λ_{ex} = 280 nm) (b) spectra recorded at room temperature for compound **1**.

dx.doi.org/10.1021/ic402718c | Inorg. Chem. 2014, 53, 3362−3370

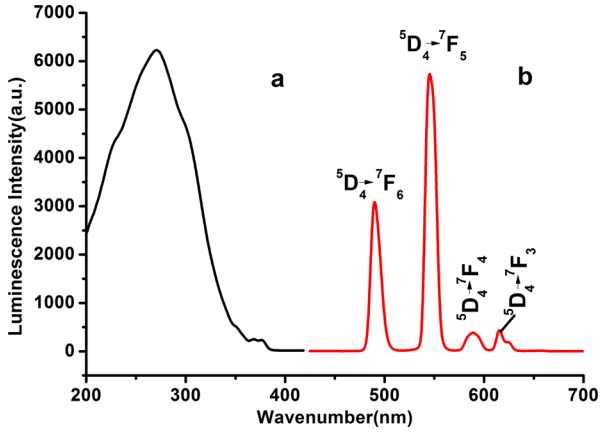

Figure 7. The solid-state excitation (λ_{em} = 545 nm) (a) and emission (λ_{ex} = 271 nm) (b) spectra recorded at room temperature for compound **2**.

broad band with peak at 272 nm in the region of 200−350 nm for the electronic transitions of the $bpdc^{2-}$ ligand and faint f−f transitions[44] at 361 nm ($^7F_0 \rightarrow ^5D_4$), 381 nm ($^7F_0 \rightarrow ^5G_2$), 392 nm ($^7F_0 \rightarrow ^5L_6$), 414 nm ($^7F_0 \rightarrow ^5D_3$), and 464 nm ($^7F_0 \rightarrow ^5D_2$) for the Eu^{3+} ion. The presence of this prominent band (272 nm) together with its higher intensity compared to the intra-$4f^6$ transitions confirms the effective sensitization of Eu^{3+} luminescence by the ligand excited states.[31] The emission spectrum (Figure 6b) of compound **1** exhibits the characteristic sharp bands centered at 594, 615, 655, and 695 nm, which are assigned to intra-$4f^6$ ($^5D_0 \rightarrow ^7F_1$, $^5D_0 \rightarrow ^7F_2$, $^5D_0 \rightarrow ^7F_3$, and $^5D_0 \rightarrow ^7F_4$) transitions of the Eu^{3+} ion (λ_{ex} = 280 nm), respectively.[45] The absence of bands from higher excited states such as $^5D_1$ in the emission spectrum implies that the nonradiative relaxation to the $^5D_0$ level is efficient.[46] The intensity of electric dipole transition ($^5D_0 \rightarrow ^7F_2$) is stronger than that of magnetic dipole transition ($^5D_0 \rightarrow ^7F_1$), implying intense red luminescence. The intensity ratio of 7.14 for $I(^5D_0 \rightarrow ^7F_2)/I(^5D_0 \rightarrow ^7F_1)$ indicates that the coordination environment of Eu^{3+} in compound **1** is lack of inversion center.[47,48]

The excitation spectrum (Figure 7a) of compound **2**, which monitored the intense characteristic emission (545 nm) of the Tb^{3+} ion, displays a notable broad band with peak at 271 nm in the range from 200 to 350 nm for the electronic transitions of the $bpdc^{2-}$ ligand and a few weak f−f transitions[32] at 352, 369, and 375 nm corresponding to the $^7F_6 \rightarrow ^5L_{10}$, $^5D_{2-3}$ intra-configurational forbidden $4f^8 \rightarrow 4f^8$ transitions for Tb^{3+}. The emission spectrum (Figure 7b) of solid compound **2** measured upon excitation at 271 nm (the maximum excitation wavelength) shows the characteristic transitions from the emitting level ($^5D_4$) to the ground multiplet ($^7F_{6-3}$) of Tb(III) ion.[49] The $^5D_4 \rightarrow ^7F_5$ transition at 545 nm is the strongest emission, implying intense green luminescence; the $^5D_4 \rightarrow ^7F_6$ transition at 489 nm is the second largest emission, while the $^5D_4 \rightarrow ^7F_4$ at 589 nm and $^5D_4 \rightarrow ^7F_3$ at 615 nm transition are the weakest in compound **2**.

It should be mentioned herein that chemists have tried a lot of ways to achieve the luminescence intensity enhancement of Ln(III) compounds by means of replacing their O−H by O−D or O−F[50] or by directly removing water molecules[3b,40,42a,42c,51,52] Fortunately, Ln^{3+} ions have their coordination spheres fully occupied by the $bpdc^{2-}$ ligands (Figure 1a) in the title compounds; that is, no water molecules enter into Ln^{3+} coordination environments. As a consequence, solid compound **1** emits strong red luminescence, and solid compound **2** emits strong green luminescence. The room-temperature excitation and emission intensity of compounds **3** and **4** are too weak to be detected, because the $bpdc^{2-}$ ligand cannot transfer energy effectively to Sm^{3+} and Dy^{3+}.

The compounds **1**−**8** are not light-sensitive under sunlight and UV light although Ag^+ ions are present, which may be due to the presence of Ln^{3+} ions and cheating to organic $bpdc^{2-}$ ligand.

The room-temperature $^5D_0$ (Eu^{3+}) and $^5D_4$ (Tb^{3+}) decay curves excited at 280 nm were recorded by monitoring the more intense $^5D_0 \rightarrow ^7F_2$ (615 nm) and $^5D_4 \rightarrow ^7F_5$ (545 nm) transitions for compounds **1** and **2**, respectively. The luminescence decay profiles (Figure 8) are single-exponential functions. The lifetime values (τ_{obs}) for compounds **1** and **2** are determined as 1.58 and 1.76 ms, respectively.[53]

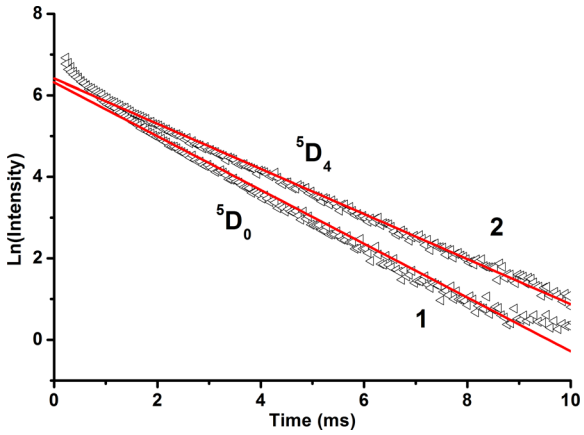

Figure 8. Emission decay profiles obtained at room temperature for compounds **1** and **2** excited at 280 nm and monitored at 615 and 545 nm, respectively.

To confirm real energy transfer efficiency between ligands and lanthanide ions, the overall quantum yield (Φ_{tot}) of ligand-sensitized lanthanide emission is calculated from the ligand sensitization efficiency (η_{sens}) and the intrinsic quantum yield (Φ_{Ln}) of the lanthanide luminescence according to the reported methods (see Supporting Information).[54,55] The radiative lifetimes (τ_R = 2.77 ms for compound **1**), intrinsic quantum yields (Φ_{Ln} = 57% for compound **1**), sensitization efficiency (η_{sens} = 36.83% for compound **1**), emission lifetimes (τ_{obs} = 1.58 ms for compound **1** and 1.76 ms for compound **2**), and overall quantum yields (Φ_{tot} = 21% for compound **1** and 22% for compound **2**) are obtained. The data show that the overall quantum yield (Φ_{tot}) and luminescence emission lifetimes (τ_{obs}) of compounds **1** and **2** are among the highest, when compared with the reported Ln-MOFs[56] and 3d−4f or 4d−4f MOFs.[50a,57]

Thermal Stability Analysis. The thermal stability of compounds **1**, **2**, and **4** selected as representative samples was examined by the thermogravimetric (TG) method (Supporting Information, Figure S7) in the temperature range from 25 to 800 °C. The compounds show remarkable good thermally stability up to 370 °C because neither aquo ligands nor lattice water molecules exist in the composition of the compounds. After 370 °C, the compounds start decomposing, with the weight loss between 370 and 500 °C

dx.doi.org/10.1021/ic402718c | Inorg. Chem. 2014, 53, 3362−3370

(60.27% for compound **1**, 61.03% for compound **2**, and 60.06% for compound **4**), corresponding to the decomposition of the organic ligands (calcd 59.96% for compound **1**, 60.19% for compound **2**, and 60.92% for compound **4**). The weight of the remaining mixed metal oxide is 39.73% for compound **1**, 38.97% for compound **2**, and 39.80% for compound **4**, which matches nicely the composition of $AgEuO_2$ (40.04%) for compound **1**, $AgTbO_2$ (39.81%) for compound **2**, and $AgDyO_2$ (39.08%) for compound **4**, respectively.

In parallel with the TG analysis, temperature-dependent XRD (Supporting Information, Figure S8) and IR (Supporting Information, Figure S9) measurements of compound **2** selected as a representive sample were also conducted after calcination at elevated temperatures to confirm the thermal stability of this material. With the increase of temperature from 200 to 370 °C, the powder XRD patterns are essentially in agreement with those of the sample without calcination (Supporting Information, Figure S8). Furthermore, in the IR spectrum of the calcined sample of compound **2**, the characteristic bands of carboxylate groups at 1594 cm^{-1} for asymmetric stretching and at 1416 cm^{-1} for symmetric stretching vibrations are identical to those of the uncalcined sample (Supporting Information, Figure S9). These phenomena suggest that the whole framework of compounds remains steady until 370 °C. Unsurprisingly, the photoluminescence of compound **1** selected as a representive sample shows negligible differences at elevated temperatures (Supporting Information, Figure S10). Therefore the title compounds are good candidates for luminescence materials requiring good thermal stability.

CONCLUSION

In summary, a new family of 3-D Ag−Ln heterometallic complexes based on the 2,2′-bipyridine-3,3′-dicarboxylate ligand have been synthesized by hydrothermal method. Compounds **1**−**8** show good thermal stability from 25 to 370 °C. The photoluminescence property study on compounds **1**−**4** demonstrates that the Eu^{3+} luminescence is well-sensitized by the $bpdc^{2-}$ ligand, indicating efficient energy transfer to Eu^{3+} and Tb^{3+}, while luminescence of Sm^{3+} and Dy^{3+} is poorly sensitized due to unmatching energy gap between the ligand triplit state of the $bpdc^{2-}$ ligand and $^4G_{5/2}$ (Sm^{3+}) and $^4F_{9/2}$(Dy^{3+}). Emission lifetimes values (τ_{obs} = 1.58 ms for compound **1** and 1.76 ms for compound **2**) and the overall quantum yields (Φ_{tot} = 21% for compound **1** and 22% for compound **2**) have been noticed. This result confirms that the use of multifunctional organic ligands containing multiple oxygen and nitrogen atoms is a good synthetic strategy for obtaining 3-D Ag−Ln heterometallic MOFs possessing good thermal stability and luminescence. Because compounds **1** and **2** have the advantages of good luminescence and thermal stability, it is expected that they may be found in applications in the luminescent materials field.

ASSOCIATED CONTENT

Supporting Information

X-ray crystallographic files in CIF format. IR spectra of the [Ag(2,2′-bipyridine)]NO_3·$5H_2O$ microtubes, the free ligand H_2bpdc and compounds **1**−**8**, compound **2** before and after calcination at elevated temperatures. SEM image of the [Ag(2,2′-bipyridine)]NO_3·$5H_2O$ microtubes. Photographic images of compound **1** selected as a representative sample. Powder X-ray diffraction patterns for the samples of compounds **1**−**9** as prepared, of compound **2** before and after calcination at elevated temperatures. Photoluminescence spectra of compound **1** measured at elevated temperatures. Photoluminescence data for reported relevant Ln-MOFs and compound **1** and **2**. The TG curves of compounds **1**, **2**, and **4**. This material is available free of charge via the Internet at http://pubs.acs.org.

AUTHOR INFORMATION

Corresponding Authors

*E-mail: zhouys@mail.buct.edu.cn (Y.Z.).
*E-mail: ljzhang@mail.buct.edu.cn (L.Z.).

Author Contributions

The manuscript was written through contributions of all authors. All authors have given approval to the final version of the manuscript.

Notes

The authors declare no competing financial interest.

ACKNOWLEDGMENTS

Financial support from the National Natural Science Foundation of China (No. 20975009, No. 21371020) is greatly acknowledged. Prof. Xue Duan of Beijing University of Chemical Technology is greatly acknowledged for his kind support.

REFERENCES

(1) Lucky, M. V.; Sivakumar, S.; Reddy, M. L. P.; Paul, A. K.; Natarajan, S. *Cryst. Growth. Des.* **2011**, *11*, 857−864.

(2) (a) Kido, J.; Okamoto, Y. *Chem. Rev.* **2002**, *102*, 2357−2368. (b) Liu, D.; Tang, K.; Liu, W.; Su, C.; Yan, X.; Tana, M.; Tang, Y. *Dalton Trans.* **2010**, *39*, 9763−9765. (c) Chen, B.; Wang, L.; Xiao, Y.; Fronczek, F. R.; Xue, M.; Cui, Y.; Qian, G. *Angew. Chem., Int. Ed.* **2009**, *48*, 500−503. (d) Austin, R. H.; Stem, D. L.; Wang, J. *Proc. Natl. Acad. Sci. USA* **1987**, *84*, 1541−1545.

(3) (a) Beeby, A.; Botchway, S. W.; Clarkson, I. M.; Faulkner, S.; Parker, A. W.; Parker, D.; Williams, J. A. G. *J. Photochem. Photobiol. B* **2000**, *57*, 83−89. (b) Cui, Y. J.; Yue, Y. F.; Qian, G. D.; Chen, B. L. *Chem. Rev.* **2012**, *112*, 1126−1162.

(4) (a) Binnemans, K. *Chem. Rev.* **2009**, *109*, 4283−4374. (b) Moore, E. G.; Samuel, A. P. S.; Raymond, K. N. *Acc. Chem. Res.* **2009**, *42*, 542−552. (c) Sabbatini, N.; Guardigli, M.; Lehn, J. M. *Coord. Chem. Rev.* **1993**, *123*, 201−228. (d) Weissman, S. I. *J. Chem. Phys.* **1942**, *10*, 214−217.

(5) Ryan, D. E; Snapeand, F.; Winpe, M. *Anal. Chim. Acta* **1972**, *58*, 101−106.

(6) (a) Dang, F. F.; Li, Y.; Liu, W. S. *Spectrochim. Acta, Part A* **2007**, *66*, 676−680. (b) Hemmilä, I. *Anal. Chem.* **1985**, *57*, 1676−1681.

(7) Ci, Y. X.; Ning, M. Z.; Yang, F. Y. *Chem. Res. Chin. Univ.* **1983**, *4*, 115−118.

(8) (a) Sakamoto, M.; Manseki, K.; Okawa, H. *Coord. Chem. Rev.* **2001**, *219*, 379−414. (b) Hasegawa, Y.; Saitou, S.; Tamaki, S.; Yajima, H.; Tadokoro, M. *Helv. Chim. Acta* **2009**, *92*, 2565−2575. (c) Dang, F.; Li, Y.; Liu, W. *Spectrochim. Acta., Part A* **2007**, *66A*, 676−680.

(9) Li, S. -M.; Zheng, X. -J.; Yuan, D. -Q.; Ablet, A.; Jin, L. -P. *Inorg. Chem.* **2012**, *51*, 1201−1203.

(10) (a) He, Y. K.; Han, Z. B. *Inorg. Chem. Commun.* **2007**, *10*, 1523−1526. (b) Qiu, Y. C.; Liu, H. G.; Ling, Y.; Deng, H.; Zeng, R. H.; Zhou, G. Y.; Zeller, M. *Inorg. Chem. Commun.* **2007**, *10*, 1399−1403. (c) Deng, H.; Li, Y. H.; Qiu, Y. C.; Liu, Z. H.; Zeller, M. *Inorg. Chem. Commun.* **2008**, *11*, 1151−1154. (d) He, Y. K.; An, H. Y.; Han, Z. B. *Solid State Sci.* **2009**, *11*, 49−55. (e) Liu, Z. H.; Qiu, Y. C.; Li, Y. H.; Deng, H.; Zeller, M. *Polyhedron* **2008**, *27*, 3493−3499. (f) Mou, J. X.; Zeng, R. H.; Qiu, Y. C.; Zhang, W. G.; Deng, H.; Zeller, M. *Inorg. Chem. Commun.* **2008**, *11*, 1347−1351.

(11) Gu, X.; Xue, D. *CrystEngComm* **2007**, *9*, 471−477.

(12) Khlobystov, A. N.; Blake, A. J.; Champness, N. R.; Lemenovskii, D. A.; Majouga, A. G.; Zyk, N. V.; Schröder, M. *Coord. Chem. Rev.* **2001**, *222*, 155−192.
(13) Ma, D. Y.; Wang, W. X.; Li, Y. W. *J. Coord. Chem.* **2010**, *63*, 448−456.
(14) Wang, N.; Yue, S.; Wu, H.; Li, Z.; Li, X.; Liu, Y. *Inorg. Chim. Acta* **2010**, *363*, 1008−1012.
(15) Zhao, X. Q.; Zhao, B.; Wei, S.; Cheng, P. *Inorg. Chem.* **2009**, *48*, 11048−11057.
(16) Zheng, Z. N.; Jang, Y. O.; Lee, S. W. *Cryst. Growth Des.* **2012**, *12*, 3045−3056.
(17) (a) Du, M.; Zhao, X. J.; Wang, Y. *Dalton Trans.* **2004**, *14*, 2065−2072. (b) Li, X.; Cao, R.; Sun, Y. Q.; Shi, Q.; Yuan, D. Q.; Sun, D. F.; Bi, W. H.; Hong, M. C. *Cryst. Growth Des.* **2004**, *4*, 255−261. (c) Du, M.; Li, C. P. *Inorg. Chim. Acta* **2006**, *359*, 1690−1696.
(18) Swamy, G. Y. S. K.; Chandramohan, K.; Lakshmi, N. V.; Ravikumar, K. *Z. Kristallogr.* **1998**, *213*, 191−194.
(19) (a) Zhong, Z. J.; You, X. Z.; Yang, Q. C. *Polyhedron* **1994**, *13*, 1951−1955. (b) Tong, M. L.; Yang, G.; Chen, X. M. *Aust. J. Chem.* **2000**, *53*, 607−610.
(20) (a) Zhang, X. M.; Wu, H. S.; Chen, X. M. *Eur. J. Inorg. Chem.* **2003**, *16*, 2959−2964. (b) Wu, B. L.; Zhang, H. Q.; Zhang, H. Y.; Wu, Q. A.; Hou, H. W.; Zhu, Y.; Wang, X. Y. *Aust. J. Chem.* **2003**, *56*, 335−338.
(21) Wu, B. L.; Yuan, D. Q.; Jiang, F. L.; Wang, R. H.; Han, L.; Zhou, Y. F.; Hong, M. C. *Eur. J. Inorg. Chem.* **2004**, *13*, 2695−2700.
(22) Guo, H. Y.; Chen, C. X.; Wei, Y. G.; Jin, X. L.; Fang, C.; Wang, P. *Chin. J. Chem.* **2004**, *22*, 816−821.
(23) (a) Hu, M.; Li, H. F.; Yao, J. Y.; Gao, Y.; Liu, Z. L.; Su, H. Q. *Inorg. Chim. Acta* **2010**, *363*, 368−374. (b) Lu, W. G.; Yang, K.; Jiang, L.; Feng, X. L.; Lu, T. B. *Inorg. Chim. Acta* **2009**, *362*, 5259−5264.
(24) Wimmer, F.; Wimmer, S. A. *Org. Prep. Proced. Int.* **1983**, *15*, 368−369.
(25) (a) Sheldrick, G. M., *SHELXTL*, V5.1, Software Reference Manual; Bruker AXS, Inc.: Madison, WI, 1997. (b) Sheldrick, W. S.; Morr, M. *Acta Crystallogr., Sect. B* **1981**, *37*, 733−734.
(26) (a) Sheldrick,G. M. *SHELXTL-97,* a Program for Crystal Structure Refinement; University of Göttingen: Gottingen, Germany, 1997. (b) Sheldrick, G. M. *SHELXS97,* Program for Crystal Structure Solution; University of Göttingen: Göttingen, Germany, 1997.
(27) Hu, M.; Wang, Q. L.; Xu, G. F.; Deng, G. R.; Yang, G. M.; Yu, M.; Zhang, Y. H. *Inorg. Chim. Acta* **2007**, *360*, 1684−1690.
(28) (a) Zhou, J. M.; Shi, W.; Xu, N. Cheng, P. *Inorg. Chem.* **2013**, *52*, 8082−8090. (b) Hu, M.; Wang, Q. L.; Xu, G. F.; Deng, G. R.; Yang, G. M. *Inorg. Chem. Commun.* **2007**, *10*, 381−384. (c) Wang, C. C.; Wang, Z. H.; Gu, F. B.; Guo, G. S. *J. Mol. Struct.* **2010**, *979*, 92−100. (d) Hu, M.; Li, H. F.; Yao, J. Y.; Gao, Y.; Liu, Z. L.; Su, H. Q. *Inorg. Chim. Acta* **2010**, *363*, 368−374. (e) Song, X. Q.; Dou, W.; Liu, W. S.; Ma, J. X. *Inorg. Chem. Commun.* **2007**, *10*, 419−422.
(29) Balaban, A. T. *J. Chem. Inf. Comput. Sci.* **1997**, *37*, 645−650.
(30) Yang, J.; Li, C. X.; Quan, Z. W.; Zhang, C. M.; Yang, P. P.; Li, Y. Y.; Yu, C. C.; Lin, J. *J. Phys. Chem. C* **2008**, *112*, 12777−12785.
(31) Su, S. Q.; Chen, W.; Qin, C.; Song, Z. Y.; Li, G. H.; Song, X. Z.; Zhu, M.; Wang, S.; Hao, Z. M.; Zhang, H. J. *Cryst. Growth Des.* **2012**, *12*, 1808−1815.
(32) Soares-Santos, P. C. R.; Cunha-Silva, L.; Almeida Paz, F. A.; Ferreira, R. A. S.; Rocha, J.; Carlos, L. D.; Nogueira, H. I. S. *Inorg. Chem.* **2010**, *49*, 3428−3440.
(33) Jia, G. H.; Law, G. L.; Wong, K. L.; Tanner, P. A.; Wong, W. T. *Inorg. Chem.* **2008**, *47*, 9431−9438.
(34) Gu, X. J.; Xue, D. F. *Cryst. Growth Des.* **2007**, *7*, 1726−1732.
(35) Law, G. L.; Wong, K. L.; Yang, Y. Y.; Yi, Q. Y.; Jia, G. H.; Wong, W. T.; Tanner, P. A. *Inorg. Chem.* **2007**, *46*, 9754−9759.
(36) Soares-Santos, P. C.R.; Cunha-Silva, L.; Paz, F.A. A.; Ferreira, R. A. S.; Rocha, J.; Trindade, T.; Carlos, L. D.; Nogueira, H. I. S. *Cryst. Growth Des.* **2008**, *8*, 2505−2516.
(37) Chen, W. T.; Fukuzumi, S. *Inorg. Chem.* **2009**, *48*, 3800−3807.
(38) Biju, S.; Ambili Raj, D. B.; Reddy, M L P; Kariuki, B M. *Inorg. Chem.* **2006**, *45*, 10651−10660.
(39) Feng, W. X.; Zhang, Y.; Zhang, Z.; Lü, X. Q.; Liu, H.; Shi, G. X.; Zou, D.; Song, J.; Fan, D. D.; Wong, W. K.; Jones, R. A. *Inorg. Chem.* **2012**, *51*, 11377−11386.
(40) Steemers, F. J.; Verboom, W.; Reinhoudt, D. N.; Vander Tol, E. B.; Verhoeven, J. W. *J. Am. Chem. Soc.* **1995**, *117*, 9408−9414.
(41) Ma, X.; Li, X.; Cha, Y. E.; Jin, L. P. *Cryst. Growth Des.* **2012**, *12*, 5227−5232.
(42) (a) Archer, R. D.; Chen, H. *Inorg. Chem.* **1998**, *37*, 2089−2095. (b) Sato, S.; Wada, M. *Bull. Chem. Soc. Jpn.* **1970**, *43*, 1955−1962.
(43) Latva, M.; Takalo, H.; Mukkala, V. M.; Matachescu, C.; Rodriguez-Ubis, J. C.; Kankare, J. *J. Lumin.* **1997**, *75*, 149−169.
(44) Tang, X. L.; Dou, W.; Chen, S. W.; Dang, F. F.; Liu, W. S. *Spectrochim. Acta, Part A* **2007**, *68*, 349−353.
(45) (a) Li, X.; Wang, C. Y.; Hu, H. M. *Inorg. Chem. Commun.* **2008**, *11*, 345−348. (b) Li, C.; Quan, Z.; Yang, J.; Yang, P. P.; Lin, J. *Inorg. Chem.* **2007**, *46*, 6329−6337.
(46) Zhang, L. J.; Xu, S.; Zhou, Y. S.; Zheng, X. R.; Yu, C.; Shi, Z. H.; Hassan, S.; Chen, C. *CrystEngComm* **2011**, *13*, 6511.
(47) Zhang, H. J.; Yan, B.; Wang, S. B.; Ni, J. Z. *J. Photochem. Photobiol., A* **1997**, *109*, 223−228.
(48) Wang, Y. B.; Zheng, X. J.; Zhuang, W. J.; Jin, L. P. *Eur. J. Inorg. Chem.* **2003**, *7*, 1355−1360.
(49) (a) Burrow, C. E.; Burchell, T. J.; Lin, P. H.; Habib, F.; Wernsdorfer, W.; Clerac, R.; Murugesu, M. *Inorg. Chem.* **2009**, *48*, 8051−8053. (b) Viswanathan, S.; Bettencourt-Dias, A. D. *Inorg. Chem.* **2006**, *45*, 10138−10146. (c) Liu, X. G.; Zhou, K.; Dong, J.; Zhu, C. J.; Bao, S. S.; Zheng, L. M. *Inorg. Chem.* **2009**, *48*, 1901−1905.
(50) (a) Li, Z. Y.; Dai, J. W.; Wang, N.; Qiu, H. H.; Yue, S. T.; Liu, Y. L. *Cryst. Growth Des.* **2010**, *10*, 2746−2751. (b) Wang, C. G.; Xing, Y. H.; Li, Z. P.; Li, J.; Zeng, X. Q.; Ge, M. F.; Niu, S. Y. *Cryst. Growth Des.* **2009**, *9*, 1525−1530. (c) Liu, M. S.; Yu, Q. Y.; Cai, Y. P.; Su, C. Y.; Lin, X. M.; Zhou, X. X.; Cai, J. W. *Cryst. Growth Des.* **2008**, *8*, 4083−4091.
(51) Bünzli, J. C. G. *Chem. Rev.* **2010**, *110*, 2729−2755.
(52) (a) Wong, K. L.; Law, G. L.; Yang, Y. Y.; Wong, W. T. *Adv. Mater.* **2006**, *18*, 1051−1054. (b) Konkowski, A. M.; Lis, S.; Pietraszkiewicz, M.; Hnatejko, Z.; Czarnobaj, K.; Elbanowski, M. *Chem. Mater.* **2003**, *15*, 656−663.
(53) de Lill, D. T.; de Bettencourt-Dias, A.; Cahill, C. L. *Inorg. Chem.* **2007**, *46*, 3960−3965.
(54) (a) Xiao, M.; Selvin, P. R. *J. Am. Chem. Soc.* **2001**, *123*, 7067−7073. (b) Comby, S.; Imbert, D.; Chauvin, A.; Bunzli, J. G.; Charbonniere, L. J.; Ziessel, R. F. *Inorg. Chem.* **2004**, *43*, 7369−7379.
(55) Werts, M. H. V.; Jukes, R. T. F.; Verhoeven, J. W. *Phys. Chem. Chem. Phys.* **2002**, *4*, 1542−1548.
(56) (a) Wang, P.; Fan, R. Q.; Liu, X. R.; Wang, L. Y.; Yang, Y. L.; Cao, W. W.; Yang, B.; WuLiJi Hasi, Q. S.; Mu, Y. *CrystEngComm* **2013**, *15*, 1931−1949. (b) Shi, J.; Hou, Y. J.; Chu, W. Y.; Shi, X. H.; Gu, H. Q.; Wang, B. L.; Sun, Z. Z. *Inorg. Chem.* **2013**, *52*, 5013−5022. (c) Ramya, A. R.; Sharma, D.; Natarajan, S.; Reddy, M. L. P. *Inorg. Chem.* **2012**, *51*, 8818−8826. (d) Amghouz, Z.; Santiago, G. G.; García, J. *Inorg. Chem.* **2012**, *51*, 1703−1716.
(57) (a) Pasatoiu, T. D.; Madalan, A. M.; Kumke, M. U.; Tiseanu, C.; Andruh, M. *Inorg. Chem.* **2010**, *49*, 2310−2315. (b) Sun, Y. G.; Gu, X. F.; Ding, F.; Smet, P. F.; Gao, E. J.; Poelman, D.; Verpoort, F. *Cryst. Growth Des.* **2010**, *10*, 1059−1067. (c) Li, S. M.; Zheng, X. J.; Yuan, D. Q.; Ablet, A.; Jin, L. P. *Inorg. Chem.* **2012**, *51*, 1201−1203. (d) Bo, Q. B.; Wang, H. Y.; Wang, D. Q.; Zhang, Z. W.; Miao, J. L.; Sun, G. X. *Inorg. Chem.* **2011**, *50*, 10163−10177.